

# Building Langmuir Probes and Emissive Probes for Plasma Potential Measurements in Low Pressure, Low Temperature Plasmas

Peixuan Li<sup>\*,1</sup>, Noah Hershkowitz<sup>\*,1</sup>, Gregory Severn<sup>\*,2</sup>

## **Corresponding Author**

#### **Gregory Severn**

severn@sandiego.edu

#### Citation

Li, P., Hershkowitz, N., Severn, G. Building Langmuir Probes and Emissive Probes for Plasma Potential Measurements in Low Pressure, Low Temperature Plasmas. *J. Vis. Exp.* (171), e61804, doi:10.3791/61804 (2021).

#### **Date Published**

May 25, 2021

#### DOI

10.3791/61804

#### **URL**

jove.com/video/61804

## **Abstract**

Langmuir probes have long been used in experimental plasma physics research as the primary diagnostic for particle fluxes (i.e., electron and ion fluxes) and their local spatial concentrations, for electron temperatures, and for electrostatic plasma potential measurements, since its invention by Langmuir in the early 1920s. Emissive probes are used for measuring plasma potentials. The protocols exhibited in this work serve to demonstrate how these probes may be built for use in a vacuum chamber in which a plasma discharge may be confined and sustained. This involves vacuum techniques for building what is essentially an electrical feedthrough, one that is rotatable and translatable. Certainly, complete Langmuir probe systems may be purchased, but they can also be built by the user at considerable cost savings, and at the same time be more directly adapted to their use in a particular experiment. We describe the use of Langmuir probes and emissive probes in mapping the electrostatic plasma potential from the body of the plasma up to the sheath region of a plasma boundary, which in these experiments is created by a negatively biased electrode immersed within the plasma, in order to compare the two diagnostic techniques and assess their relative advantages and weaknesses. Although Langmuir probes have the advantage of measuring the plasma density and electron temperature most accurately, emissive probes can measure electrostatic plasma potentials more accurately throughout the plasma, up to and including the sheath region.

# Introduction

During this first century of plasma physics research, dating from Langmuir's discoveries in the 1920s of the medium like behavior of a new state of matter, plasma, the Langmuir probe has proved to have been the single most important diagnostic of plasma parameters. This is true in part, because of its extraordinary range of applicability<sup>1</sup>. In plasma

<sup>&</sup>lt;sup>1</sup> Department of Engineering Physics, University of Wisconsin <sup>2</sup> Department of Physics & Biophysics, University of San Diego

<sup>\*</sup>These authors contributed equally



encountered by satellites<sup>2,3,4</sup>, in semiconductor processing experiments, 5,6,7,8 at the edges of plasma confined in tokamaks, 9,10,11 and in wide range of basic plasma physics experiments, Langmuir probes have been used to measure plasma densities and temperatures spanning the ranges  $10^8 \le n_e \le 10^{19} m^{-3}$ , and  $10^{-3} \le T_e \le 10^2 eV$ , respectively. Simultaneously in the 1920s, he invented the probe now named after him and the emissive probe 12. The emissive probe is now primarily used as a diagnostic of plasma potential. Although it cannot measure the breadth of plasma parameters that the Langmuir probe can, it too is a diagnostic of wide utility when it comes to the measurement of plasma potential, or, as it is sometimes called, the electrostatic space potential. For example, the emissive probe can accurately measure space potentials even in a vacuum, where Langmuir probes are incapable of measuring anything.

The basic setup of the Langmuir probe consists of putting an electrode into the plasma and measuring the collected current. The resulting current-voltage (I-V) characteristics can be used to interpret plasma parameters such as electron temperature  $T_e$ , electron density  $n_e$ , and plasma potential  $\phi^{13}$ . For a Maxwellian plasma, the relationship between collected electron current  $I_e$  (taken to be positive) and probe bias  $V_B$  can be expressed as  $^{14}$ :

$$I_e(V_B) = \begin{cases} I_{e0} exp[\frac{e(V_B - \phi)}{KT_e}] &, \qquad V_B \leq \phi \\ I_{e0} &, \qquad V_B > \phi \end{cases} \tag{1a}$$

where le0 is the electron saturation current,

$$I_{e0} = Sn_e^{\infty} e \sqrt{T_e/2\pi m_e} , \qquad (2)$$

and where S is the collecting area of the probe,  $n_e^{\infty}$  is the bulk electron density, e is the electron charge,  $T_e$  is the electron temperature,  $m_e$  is the electron mass. The theoretical relation

of I-V characteristics for the electron current is illustrated in two ways in **Figure 1A** and **Figure 1B**. Note, Eq. (1a,b) only applies to bulk electrons. However, Langmuir probe currents can detect flows of charged particles, and adjustments must be made in the presence of primary electrons, electron beams, or ion beams etc. See Hershkowitz<sup>14</sup> for more details.

The discussion here takes up the ideal case of Maxwellian electron energy distribution functions (EEDF). Of course, there are many circumstances in which non-idealities arise, but these are not the subject of this work. For example, in materials processing etching and deposition plasma systems, typically RF generated and sustained, there are molecular gas feed stocks that produce volatile chemical radicals in the plasma, and multiple ion species including negatively charged ions. The plasma becomes electronegative, that is, having a significant fraction of the negative charge in the quasineutral plasma in the form of negative ions. In plasma with molecular neutrals and ions, inelastic collisions between electrons and the molecular species can produce dips<sup>15</sup> in the currentvoltage characteristics, and the presence of cold negative ions, cold relative to the electrons, can produce significant distortions 16 in the vicinity of the plasma potential, all of which of course are non-Maxwellian features. We prosecuted the experiments in the work discussed in this paper in a single ion species noble gas (argon) DC discharge plasma, free of these kinds of non-Maxwellian effects. However, a bi-Maxwellian EEDF is typically found in these discharges, caused by the presence of secondary electron emission <sup>17</sup> from the chamber walls. This component of hotter electrons is typically a few multiples of the cold electron temperature, and less than 1% of the density, typically easily distinguished from the bulk electron density and temperature.



As  $V_B$  becomes more negative than  $\phi$ , electrons are partially repelled by the negative potential of the probe surface, and the slope of the  $ln(l_e)$  vs.  $V_B$  is  $e/T_e$ , ie.  $1/T_eV$  where  $T_eV$  is the electron temperature in eV, as shown in **Figure 1B**. After  $T_{eV}$  is determined, the plasma density can be derived as:

$$n_e^{\infty} = \frac{l_{e0}}{Se} \sqrt{\frac{2\pi m_e}{T_e}} = 3.74 \times 10^{13} \frac{l_{e0}}{ST_{eV}} m^{-3}$$
 (3)

Ion current is derived differently than electron current. Ions are assumed to be "cold" due to their relatively large mass, M<sub>i</sub> >> m<sub>e</sub>, compared to that of the electron, thus, in a weakly ionized plasma, the ions are in fairly good thermal equilibrium with the neutral gas atoms, which are at the wall temperature. lons are repelled by the probe sheath if  $V_B \ge \phi$  and collected if  $V_B < \phi$ . The collected ion current is approximately constant for negatively biased probes, while the electron flux to the probe decreases for probe bias voltages more negative than the plasma potential. Since the electron saturation current is much larger than the ion saturation current, the total current collected by the probe decreases. As the probe bias becomes increasingly negative, the drop in current collected is great or small as the electron temperature is cold or hot, as described above in Eq. (1a). The equation for ion current in this approximation is:

$$I_i(V_B) = \begin{cases} I_{i0} & V_B < \phi \\ 0 & V_B > \phi \end{cases} \tag{4}$$

where

$$I_{i0} \approx -\frac{1}{2}eSn_0u_B \tag{5}$$

and

$$u_B = \sqrt{\frac{T_{ev}}{M_i}} \tag{6}$$

We note that constant ion flux collected by the probe exceeds the random thermal ion flux due to acceleration along the presheath of the probe and thus ions reach the sheath edge of the probe at the Bohm speed<sup>18</sup>, uB, rather than the ion thermal speed<sup>19</sup>. And the ions have a density equal to the electrons since the presheath is quasineutral. Comparing the ion and electron saturation current in Eqn.5 and 2, we observe that the ion contribution to the probe current is smaller than that of electrons by a factor of  $\sqrt{M_i/2\pi m_e}$ . This factor is about 108 in the case of argon plasma.

There is a sharp transition point where the electron current goes from exponential to a constant, known as the "knee". The probe bias at the knee can be approximated as the plasma potential. In the real experiment, this knee is never sharp, but rounded due to the space-charge effect of the probe, that is, the expansion of the sheath surrounding the probe, and also to probe contamination, and plasma noise<sup>13</sup>.

The Langmuir probe technique is based on collection current, whereas the emissive probe technique is based on the emission of current. Emissive probes measure neither temperature nor density. Instead they provide precise plasma potential measurements and can operate under a variety of situations due to the fact that they are insensitive to plasma flows. The theories and usage of emissive probes are fully discussed in the topical review by Sheehan and Hershkowitz<sup>20</sup>, and references therein.

For plasma density  $10^{11} \le n_e \le 10^{18}$  m<sup>-3</sup>, the inflection point technique in the limit of zero emission is recommended, which means to take a of series of I-V traces, each with different filament heating currents, finding the inflection point bias voltage for each I-V trace, and extrapolate the inflection



points to the limit of zero emission to get the plasma potential, as shown in **Figure 2**.

It is a common assumption that Langmuir and emissive probe techniques agree in quasineutral plasma, but disagree in the sheath, the region of the plasma in contact with the boundary in which space-charge appears. The study focuses on the plasma potential near plasma boundaries, in low temperature, low pressure plasma in an effort to test this common assumption. To compare potential measurements by both Langmuir probe and emissive probe, plasma potential is also determined by applying inflection point technique to Langmuir probe I-V, as shown in Figure 3. It is generally accepted<sup>1</sup> that the plasma potential is found by finding the probe bias voltage at which the second derivative of the current collected differentiated with respect to the bias voltage,  $d^2I/dV^2 = 0$ , that is, the peak of the dI/dV curve, with respect to the probe bias voltage. Figure 3 demonstrates how this maximum in dI/dV, the inflection point of the currentvoltage characteristic, is found.

Langmuir probes (collecting) and emissive probes (emitting) have different I-V characteristics, which also depend on the geometry of the probe tip, as shown in **Figure 4**. The space-charge effect of the probe must be considered before the probe fabrication. In the experiments, for the planar Langmuir probes, we used a  $\frac{1}{4}$ " planar Tantalum disk. We could collect more current and get bigger signals with a larger disk. However, in order for the analyses above to apply, the area of the probe,  $A_p$  must be kept smaller than the electron loss area of the chamber,  $A_W$ , satisfying<sup>21</sup> the inequality  $A_p \leq A_W$ . For the cylindrical Langmuir probe, we used a 0.025 mm thick, 1 cm long Tungsten wire for the cylindrical Langmuir probe and a same thickness for the Tungsten wire for the emissive probe. It is important to note that for cylindrical Langmuir

probes, for the plasma parameters of these experiments, the radius of the probe tip,  $r_p$ , is much smaller than its length,  $L_p$ , and smaller than the Debye length,  $\lambda_D$ ; that is,  $r_p \ll L_p$ , and  $0 < r_p/\lambda_D < 1$ . In this range of parameters, applying Orbital Motion Limited theory and Laframboise's development of it<sup>22</sup> for the case of thermal electrons and ions, we find that for probe bias voltages equal to or greater than the plasma potential, the electron current collected may be parameterized by a function of the form  $I_e = I_{eo}(1 + V_B/T_{eV})^{C_e}$ , where the exponent  $C_e \sim 0.4$ . The important point here is that for values of this exponent less than unity, the inflection point method for determining the plasma potential, as described in the paragraph above, applies to cylindrical Langmuir probes too.

## **Protocol**

# 1. Building Langmuir probes and Emissive probes to fit into a vacuum chamber

- 1. Planar Langmuir probe (see Figure 5 for more details)
  - Take a ¼" diameter stainless steel tube as the probe shaft and bend one end to the desired 90° angle.
  - Cut the unbent side to a length so that the probe can axially cover more than half of the chamber length.
  - Fit the unbent side of the shaft through the brass tube by a SS-4-UT-A-8 adapter in combination with a B-810-6 union tube fitting.
  - Use a ½" brass tube extending out of the customized flanges through a B-810-1-OR swagelok interface to provide axial support for the probe shaft.
  - Connect the unbent end of the probe shaft to the BNC housing through a B-400-1-OR swagelok fitting, as shown in Figure 6.



- 6. Fit the gold-coated nickel wire through two single-bore alumina tubes (1/8" and 3/16" in diameter) with the thicker one fits inside the probe shaft, as shown in **Figure 7**.
- Spot weld one end of gold-coated nickel wire onto a
  piece of stripped wire, which is soldered onto the pin
  of the BNC feedthrough at the end of the probe shaft.
- Cut the gold-coated wire to length such that the joint with the stripped wire fits inside the alumina tube to prevent short circuit with the probe shaft.
- Punch through a tantalum sheet to make a planar Langmuir probe tip (¼" in diameter)
- 10. Spot weld the other end of the gold-coated nickel wire onto the edge of the probe tip and set the probe tip to be normal to the axis of the boundary plate.
- 11. Position the probe tip a little forward so that the body of the probe does not touch the boundary plate while taking measurements inside the sheath.
- 12. Seal all joints with ceramic paste (e.g., Sauereisen Cement No. 31) to insulate the probe circuit components from plasma. Use a heat gun to bake the ceramic joints for 5-10 min.
- 13. Use a multimeter to measure the resistance between the probe tip and the BNC connector. If continuity is demonstrated, the probe is ready to be put into the vacuum chamber.
- Building a cylindrical emissive probe (see Figure 8 for more details)
  - Follow step 1.1.1-1.1.4 and repeat step 1.1.5-1.1.7
     on the same probe shaft twice with the exception
     of using a 1/8", two-bore alumina tube instead of a
     single-bore one.

- 2. Cut the 0.025 mm diameter tungsten wire to about 1 cm.
- Spot weld the tungsten filament onto gold-coated wires.
- Seal all the joints with ceramic paste and make sure the ceramic paste does not get onto the tungsten filament.
- 5. Check continuity between two BNC ends.

# 2. Generate plasma

- Turn on the ion gauge to check the base pressure before putting gas into the chamber. Proceed with zeroing of the baratron gauge if the pressure is in the low 10<sup>-6</sup> Torr range. Otherwise, check the leak in the system. The positions of needle valve and the shut off value are open and closed, respectively.
- Use a plastic screwdriver to calibrate the baratron display until the number floats between ±0.01 mTorr.
- Close the needle valve so that it is gently seated in a closed position.
- 4. Open the shutoff valve. Check that there is no pressure change on the baratron reading.
- 5. Slowly turn the knob of the needle valve to release the gas into the chamber until the pressure reaches the requirement for the experiment. The typical working pressure stem from  $10^{-5} \sim 2 \times 10^{-3}$  Torr. Working gases have included argon, xenon, krypton, oxygen etc.
- 6. Turn on the KEPCO voltage power supply and set the voltage to -60 Volts to provide sufficient electron energy for the maximum ionization cross section of argon. Turn on the heating power supply for the filaments and slowly adjust the level until the discharge current reads the



- required value. The discharge current tends to drop quickly in the first few minutes. Keep adjusting the current level for about 30 minutes until the discharge stabilizes
- Connect the voltage supply to the boundary plate and adjust the bias to desired level.

## 3. Take measurements

NOTE: I-V traces for Langmuir probes and emissive probes are acquired by a 16-bit DAQ board controlled by a Labview program. The details are not presented here since different users have different preferences for taking the data. However, there is a protocol for how to use the probes.

 Take the load line: obtain an I-V trace without any plasma discharge in the chamber with all connections made between the probe and its measuring circuit (see Figure 9, Figure 10 & Figure 11 for the UW-Madison and the USD setup).

## 2. Langmuir probes

- Clean the probe tip (this step is critical, as a clean probe exhibits a sharper 'knee' than a dirty probe) by biasing the probe positively to collect a large electron current.
  - Draw a current through the probe with a variable power supply and 50 Ohms to the machine ground to heat the tip so as to evaporate the layer of impurities that immediately attaches to the probe surface in the plasma and increase the surface resistivity of the probe.
  - Slowly increase the bias positively to surpass the plasma potential, permitting the probe to begin to draw the electron saturation current.

- Continue to raise the potential; once one sees
  the probe tip glowing cherry red, the probe is
  clean. It is necessary to have a view of the probe
  tip in the plasma through a vacuum viewport.
- 4. Be careful and vigilant while varying the bias on the probe. If the probe is allowed to get too hot, the probe tip itself could become warped, and worse things can happen, such as the tip could have holes in it, it could evaporate, it could fall off; wires could melt and lose their insulation, and so forth.
- 5. Attach the probe to the data acquisition and control circuit (this is the part that will vary from lab to lab), and proceed to sweep the voltage applied to the probe while simultaneously measuring the current drawn by the probe. Save the I-V trace.
- Attach the probe to the data acquisition and control circuit (this is the part that will vary from lab to lab), and proceed to sweep the voltage applied to the probe while simultaneously measuring the current drawn by the probe. Save the I-V trace.

## 3. Emissive probes

 Repeat step 3.2.2 with the emissive probe's data acquisition and control circuit.

## 4. Data analysis

- Langmuir Probes (See Figure 12, Figure 13 for more details).
  - Subtract the load line from the total I-V characteristic.
  - 2. Fit the ion saturation current and subtract from the remaining I-V characteristics.



- Take the natural log of current and plot it against the probe voltage.
- Take linear fits of transitional region and saturation current separately.
- Take the inverse of the slope of the transitional region and obtain the electron temperature value.
- Obtain the plasma density by plugging the current at the crossing where the two fitted lines cross each other into Eq.3.
- Apply the inflection point technique to the Langmuir probe trace and determine the plasma potential.
- 2. Emissive Probe (refer to Figure 2).
  - Repeat step 4.1.1-4.1.2 for individual I-V characteristics, then smooth each trace.
  - Differentiate each I-V trace and apply appropriate smoothing.
  - Locate the peak of each smoothed dl/dV (inflection point).
  - 4. Apply a linear fit to the inflection points.
  - Obtain the plasma potential by locating the zero crossing of the fitted line.

# **Representative Results**

Langmuir probes, known to be sensitive to flows and to the kinetic energy of the particles they collect, have up till now have been considered to yield valid measurement of the plasma potential, except in sheaths. But direct comparisons of plasma potentials measured by Langmuir probes and emissive probes have demonstrated that in the quasineutral presheath region of the plasma immediately in contact with the sheath on the plasma side, Langmuir probes do not provide accurate measurements of the plasma potential<sup>23</sup>.

Plasma potentials from plasma bulk into the sheath measured by four different types of Langmuir probes were compared with the ones measured by an emissive probe for four different neutral pressures. Langmuir probes were built in four different configurations (see **Figure 14**) and were labeled as LP<sub>j</sub> with j being an integer from 1 to 4. The cylindrical Langmuir probe is LP<sub>1</sub>, LP<sub>2</sub>, the double sided Langmuir probe, LP<sub>3</sub>, the planar Langmuir probe with the side facing the boundary plate sealed by ceramic paste, and LP<sub>4</sub> stands for the planar Langmuir probe with the side facing away from the boundary plate covered by ceramic plate. The comparison between Langmuir probes and emissive probe potential measurements are shown in **Figure 15**.

It is well known that in the presheath, ions flow toward the boundary in order to set up the sheath structure, and that the speed of the ion flow ranges zero to the Bohm speed 18,20,21. We attempted to find out experimentally (see Figure 16C for the experimental setup) whether Langmuir probes used to measure plasma potentials give accurate results in the presheath. Plasma parameters such as Temperature, density, Debye lengths and Child-Langmuir sheath lengths, calculated from measurements by LP2 in the bulk of the plasma, are shown in Table 1. As mentioned above, we tried different designs of Langmuir probes, ones that were insulating on one side or the other, as well as that were conducting on both faces of the disc. We compared all the Langmuir probe measurements to emissive probe measurements of the plasma potential. We found that all of the Langmuir probes measured plasma potentials that deviated from that measured by emissive probes in the presheath, with a difference that is positive relative to the plasma potential measured by emissive probes. The difference widens with proximity to the sheath edge, growing to a value of many electron temperatures. The difference



becomes apparent at a distance of three or four sheath thickness from the boundary. Representative results are shown in **Figure 15A-C**. This difference is an important result.

It shows the commonly held assumption is not generally the case.

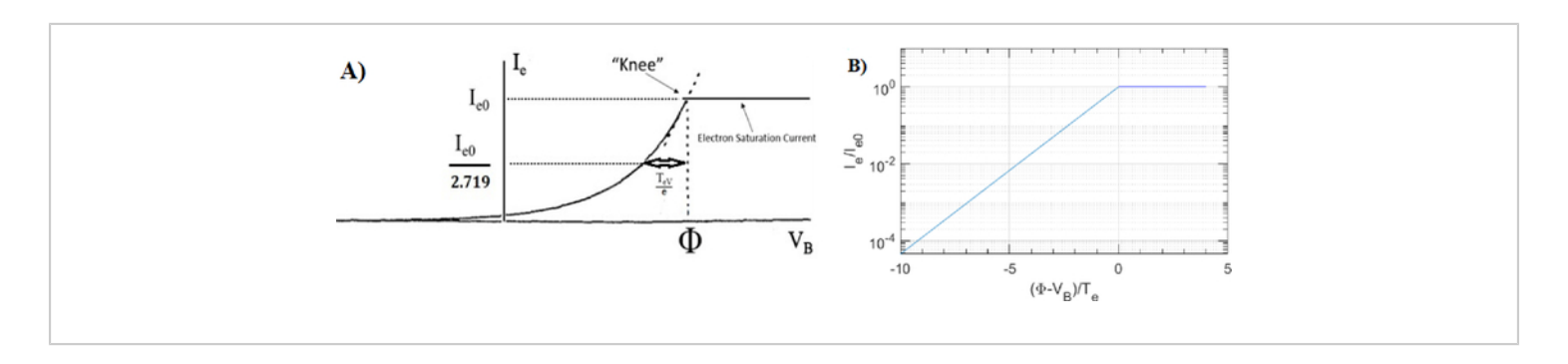


Figure 1: Electron current collected by planar Langmuir probes. Ideal electron current ( $I_e$ ) versus probe bias ( $V_B$ ) considering only bulk electrons are present in thermodynamic equilibrium at temperature  $T_{eV}$  and plotted with vertical axes as (**A**) linear and (**B**) logarithmic. Note that this data is acquired by subtracting the ion current from the probe current. The plasma potential is indicated by  $\phi$ . Please click here to view a larger version of this figure.

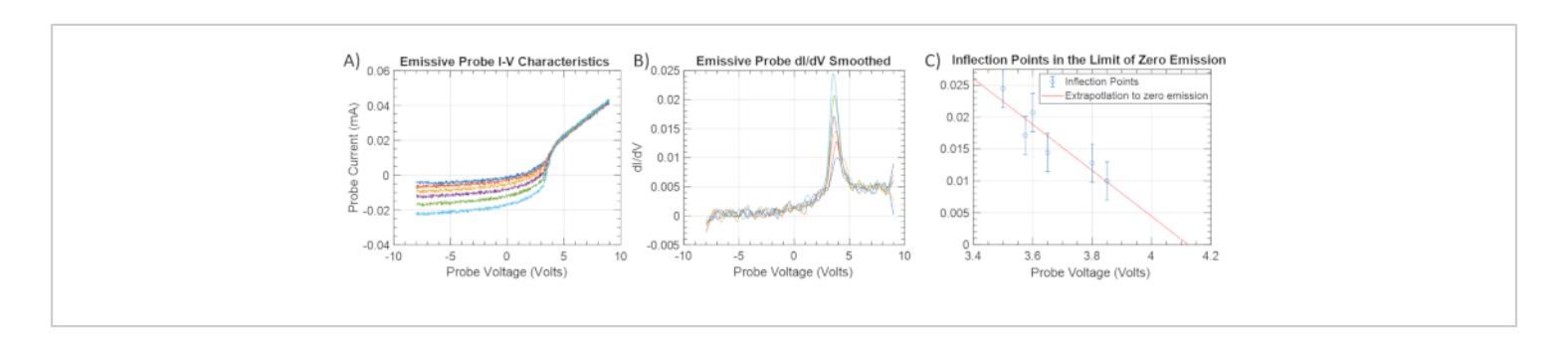


Figure 2: Emissive probe current - voltage characteristics and inflection point techniques. A) A sample set of I-V traces by emissive probe in the linear scale and B) smoothed dI/dV curves. C) The plasma potential is determined by taking the inflection point in the limit of zero emission Please click here to view a larger version of this figure.



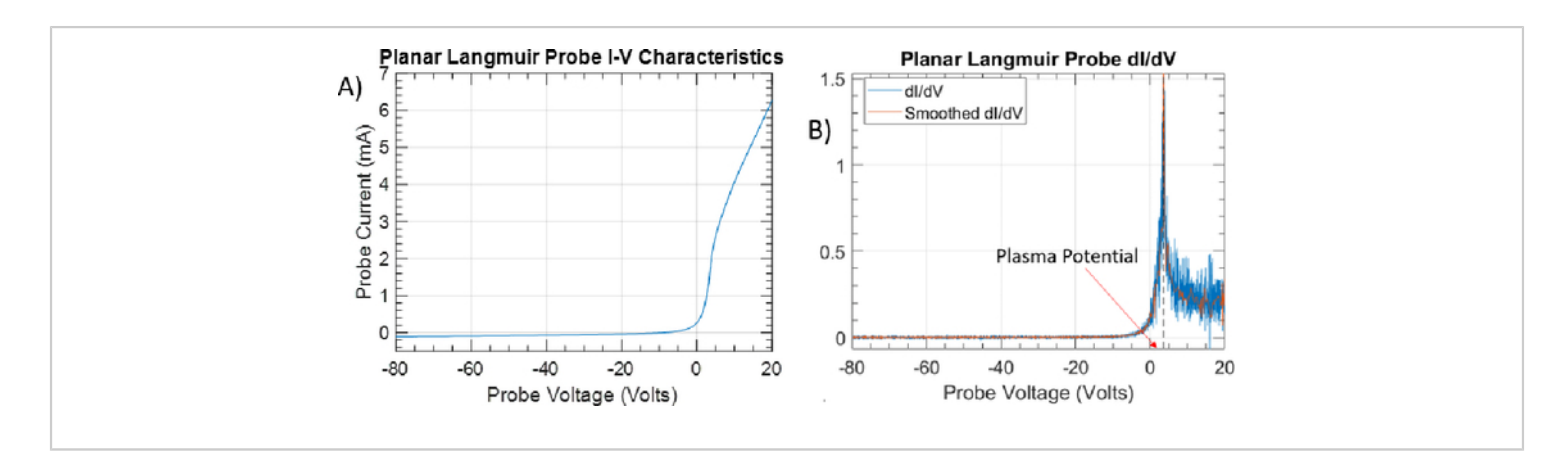


Figure 3: Langmuir probe current-voltage characteristic and inflection technique for plasma potential measurement. Plasma potential determined from the A) Langmuir probe I-V trace by B) inflection point method Please click here to view a larger version of this figure.

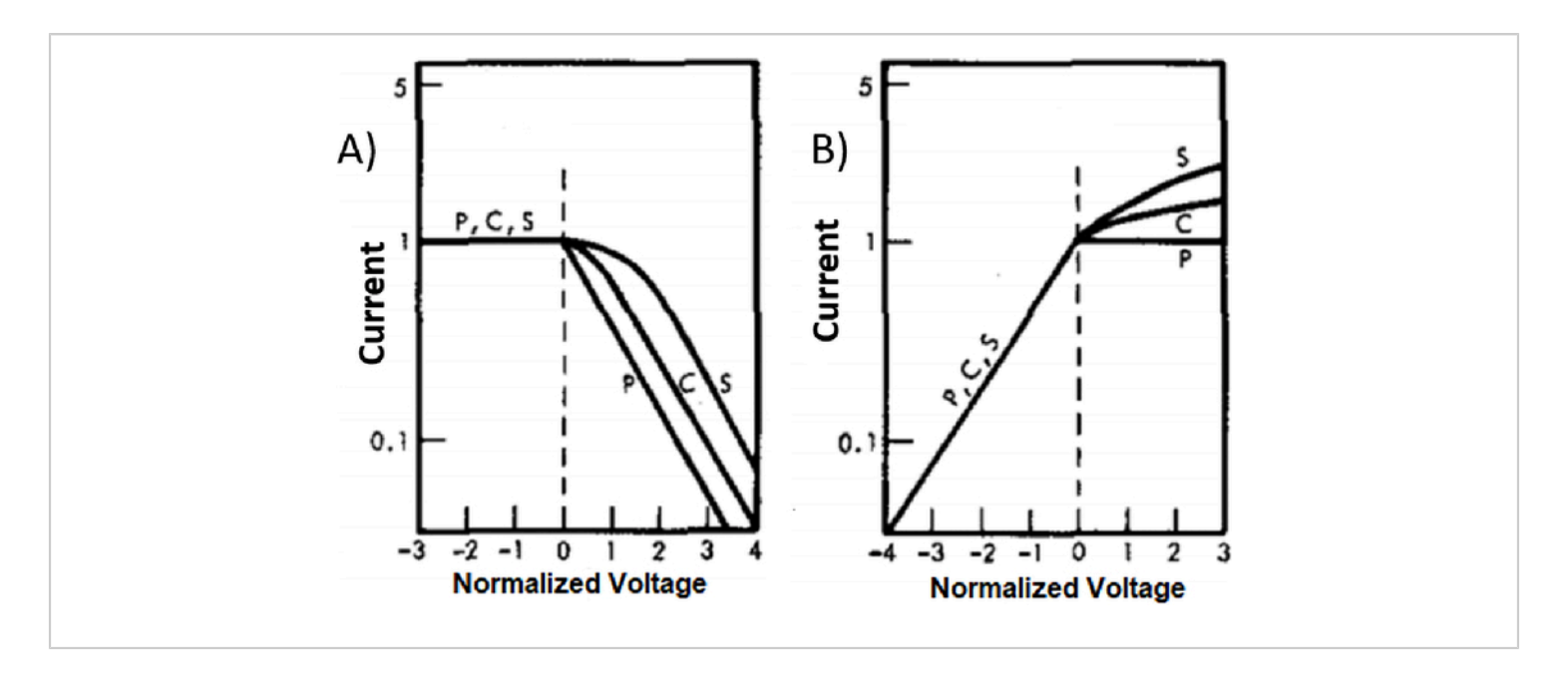
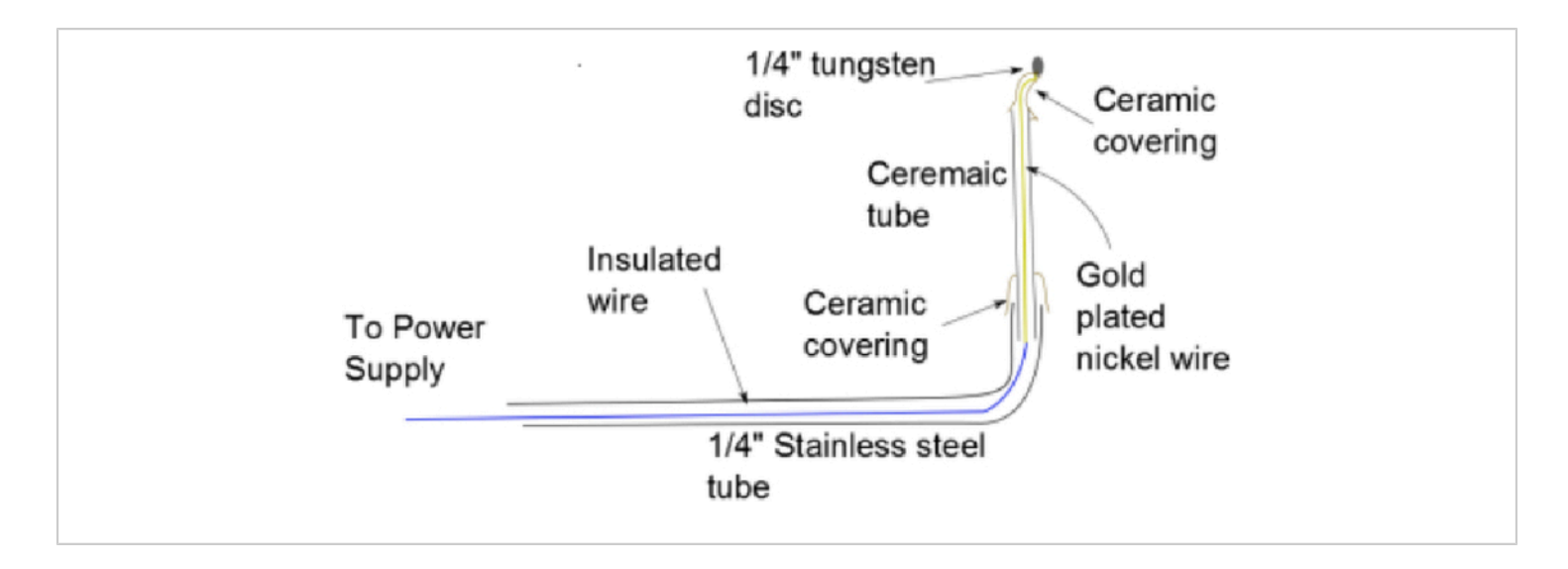
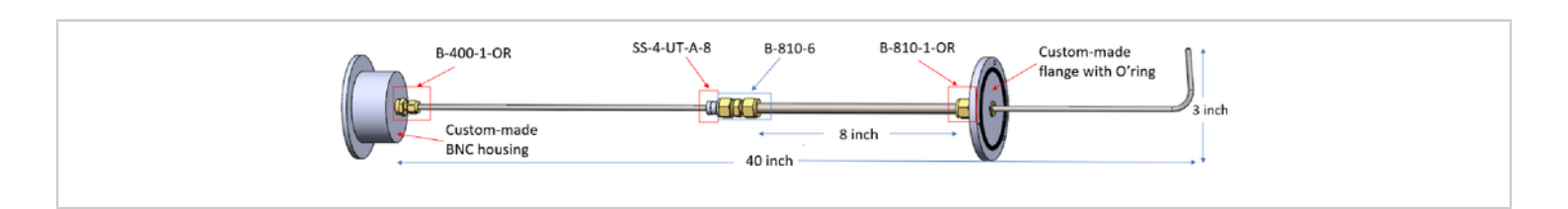


Figure 4: Sheath expansion characteristics for planar, cylindrical, and spherical Langmuir probe tips for the case of collection and emission. Normalized I-V characteristics for the A) collecting probes and B) the emitting probes with different tip geometries (planar, cylindrical, and spherical). This figure has been modified from Sheehan and Hershkowitz<sup>20</sup>. Please click here to view a larger version of this figure.





**Figure 5: Planar Langmuir probe tip mechanical schematic.** A tungsten or tantalum tip is spot welded onto the wire (gold-plated nickel wire) exposed beyond the ceramic tubing. Ceramic past fastens the ceramic tubing to the stainless-steel tubing. Please click here to view a larger version of this figure.



**Figure 6: Langmuir probe body.** Shown with part numbers and dimensions, the Langmuir probe body is design for vacuum seals at the vacuum chamber wall, at the coax cable connector (not shown here, see **Supplement Figure 6**), and a sliding, rotatable vacuum seal against the probe shaft. All tube fittings are listed in the table of materials. Please click here to view a larger version of this figure.



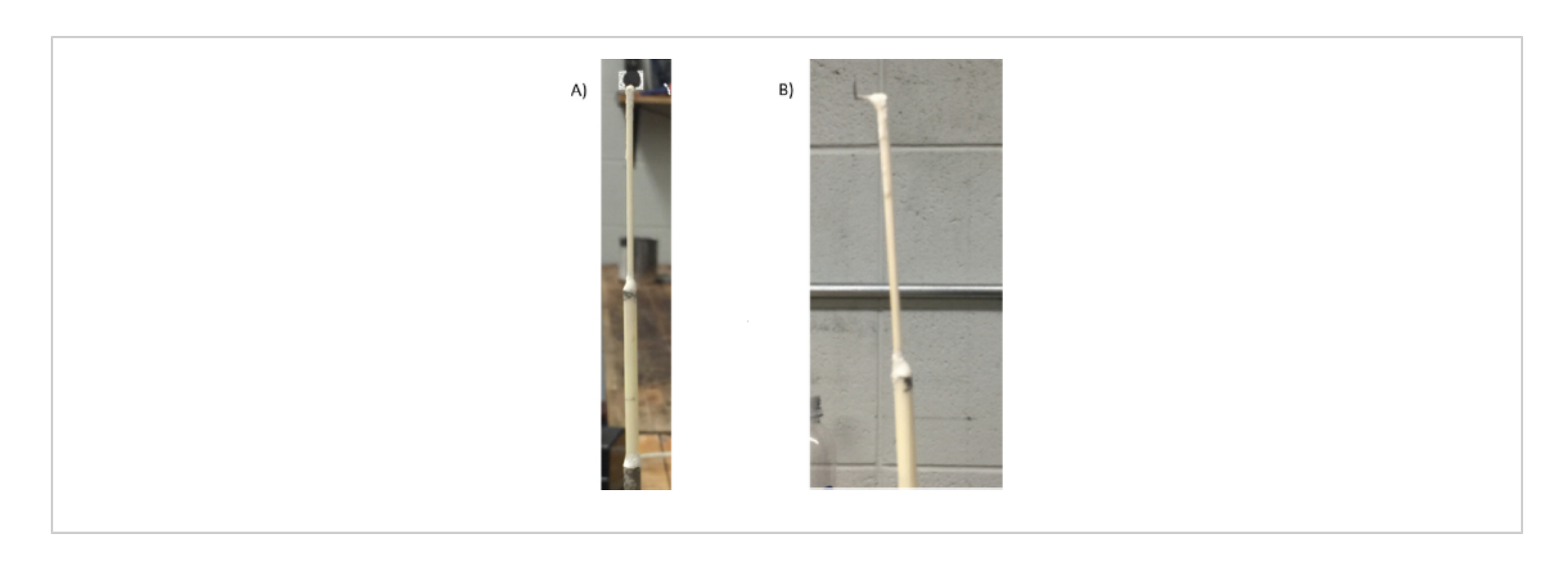


**Figure 7: Views of Langmuir probe tip fabrication and connection to probe shaft. A)** Back View and **B)** side view of planar Langmuir probe. The probe tip is spot-welded to the gold-coated nickel wire which goes through two alumina tubes with the thicker one fitted in the metal shaft. All joints are sealed with ceramic paste.



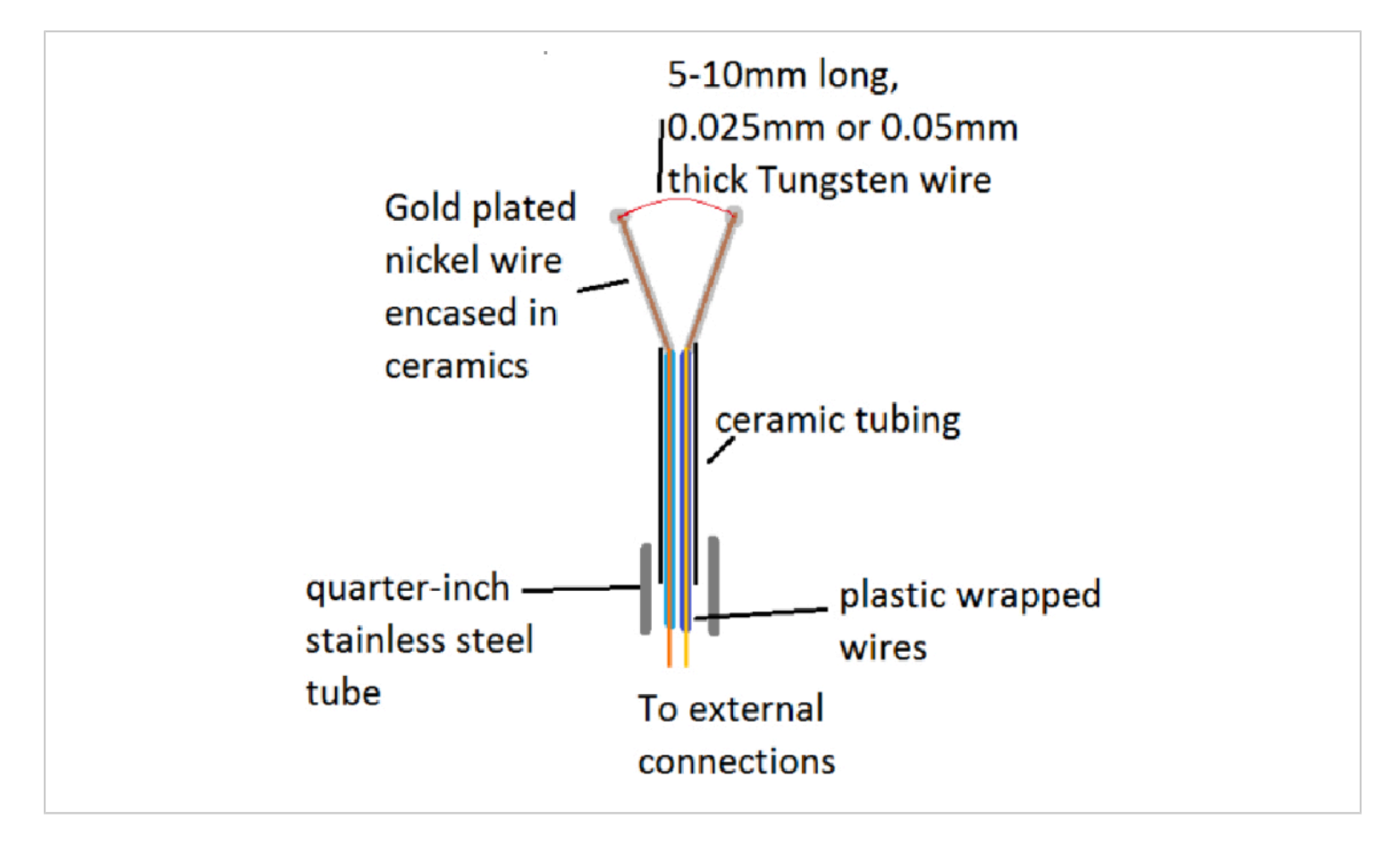


**Figure 8: Emissive probe tip schematic.** Similar to Langmuir probe fabrication, the filament (tungsten wire) is spot welded to the gold plated nickel wire protruding from the small ceramic tubing covering each stalk. Ceramic past covers the exposed nickel wire and spot-weld, and fastens the ceramic tubing together and to the stainless steel tubing. Please click here to view a larger version of this figure.



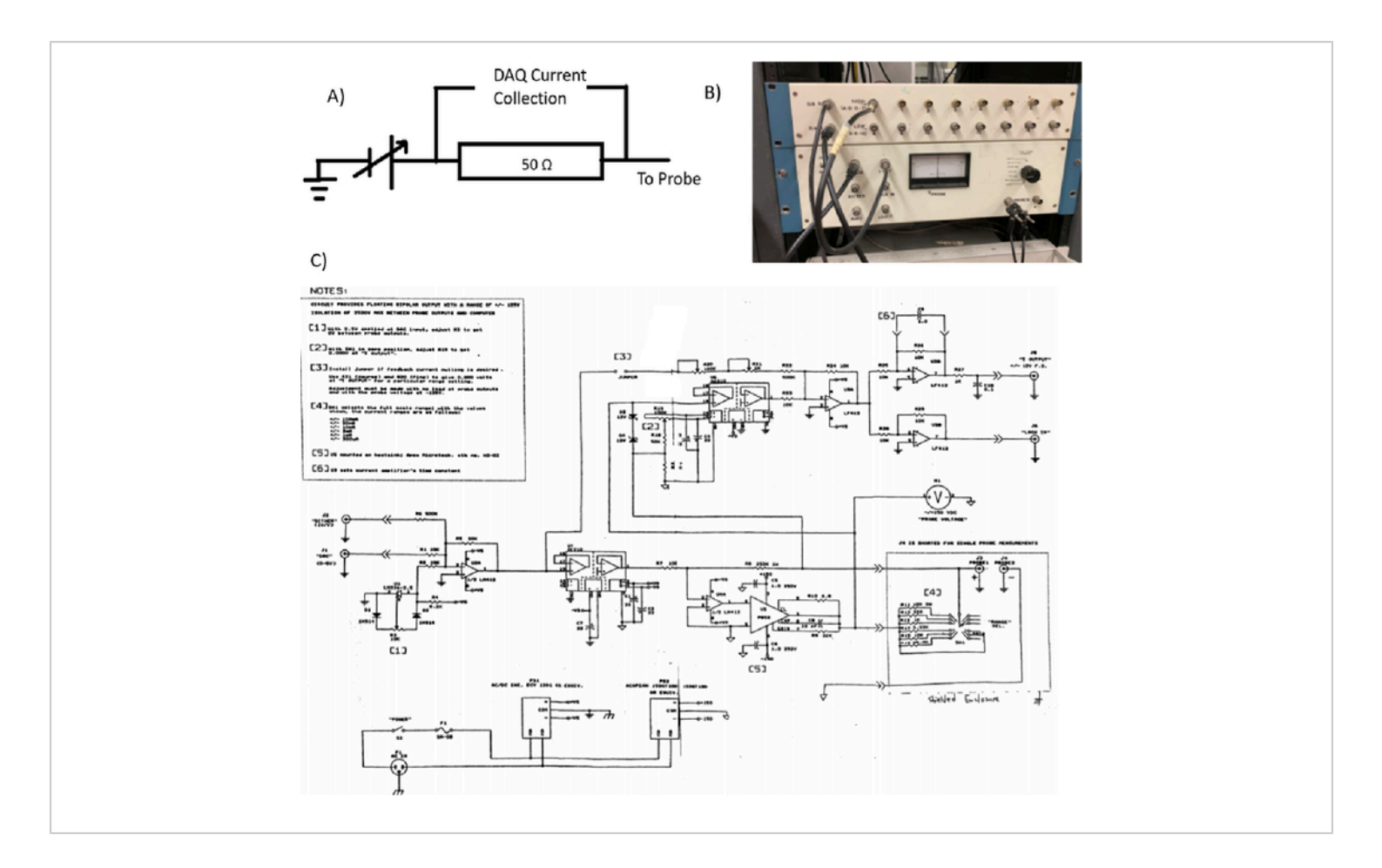


**Figure 9: Langmuir probe measurement circuits at UW-Madison. A**) A simplified measurement circuit for a Langmuir probe, **B**) The custom built DAQ and DAC board used at UW-Madison, and **C**) its circuit diagram. Please click here to view a larger version of this figure.



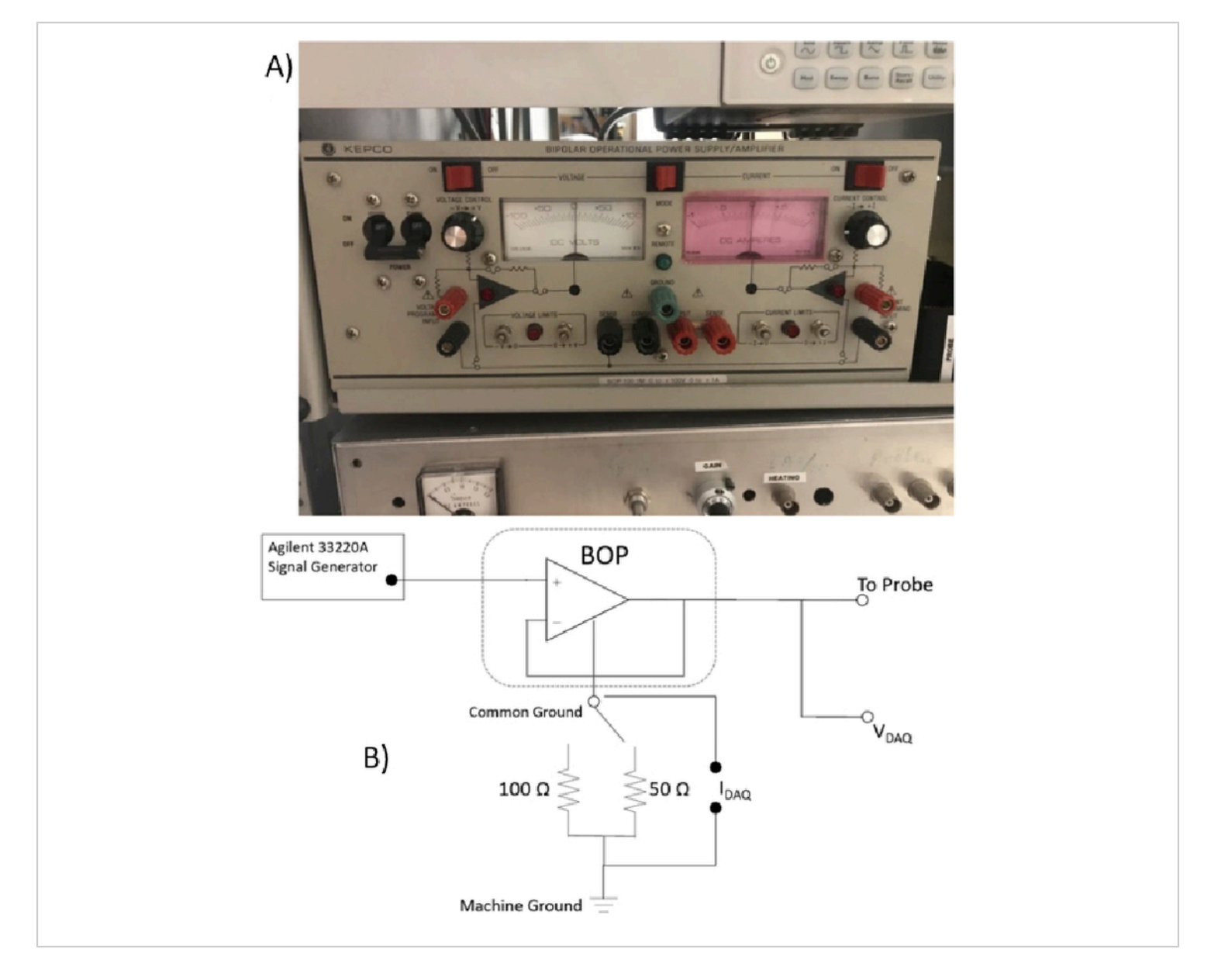


**Figure 10: Langmuir probe measurement circuits at USD.** The bipolar operational amplifier power supply (4 quadrant power supply) and home built circuit to interface with 16-bit DAQ controlled by computer scripts, used at the USD. Please click here to view a larger version of this figure.



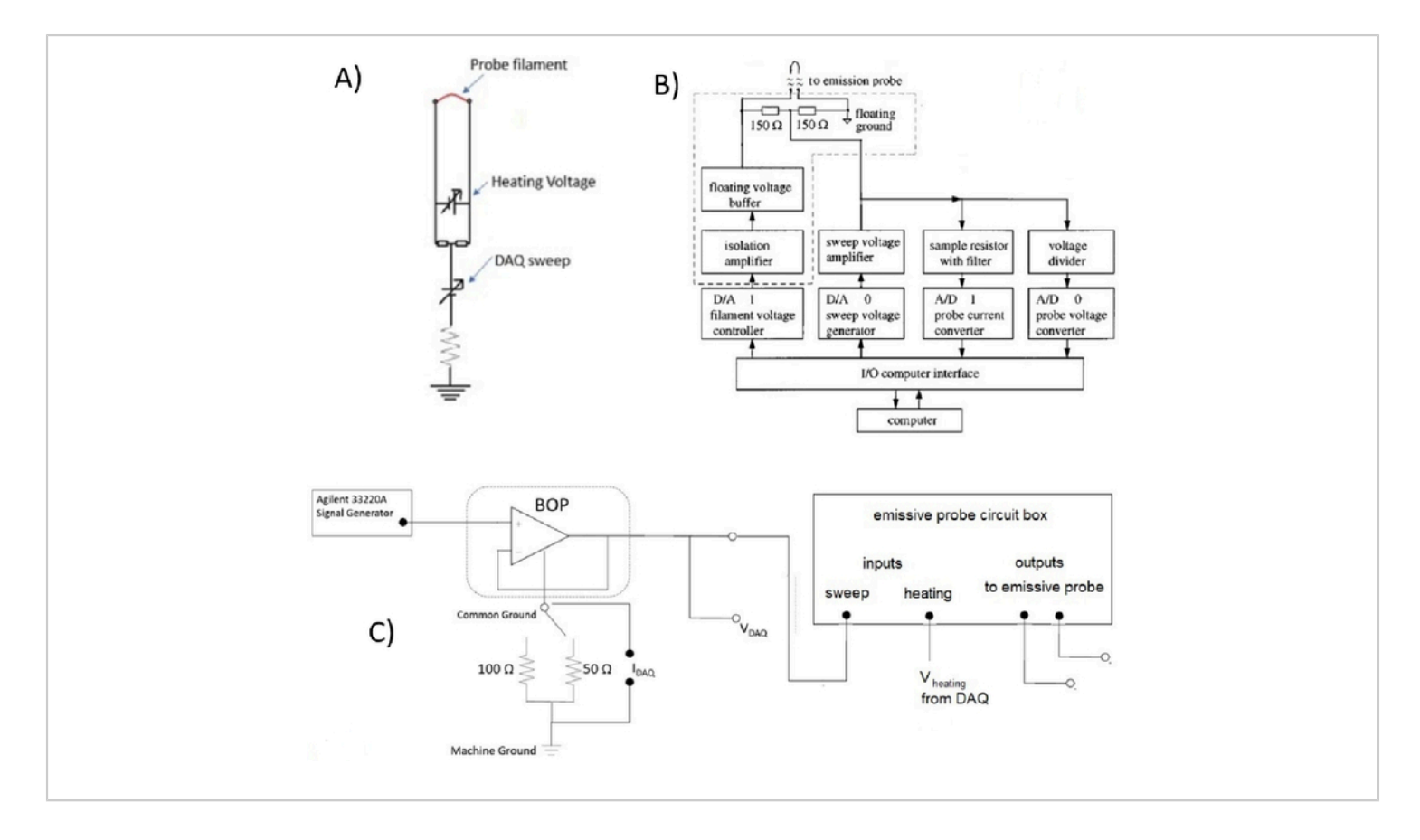


**Figure 11: Emissive probe measurement circuits at UW-Madison and USD.** (**A**) A simplified measurement circuit diagram for the emissive probe, along with (**B**) a block diagram for the heating circuit used for emissive probes at both UW-Madison and USD. The heating circuit is described in more detail in Yan S-L et al.<sup>26</sup>, from which this figure is adapted. The dotted line indicates the emissive probe circuit box, which has two inputs, one for the heating voltage and one for the sweep voltage, and two outputs, for BNC cables that connect to the emissive probe. An interface circuit between the heating circuit and the DAQ used at USD, in (**C**). Please click here to view a larger version of this figure.



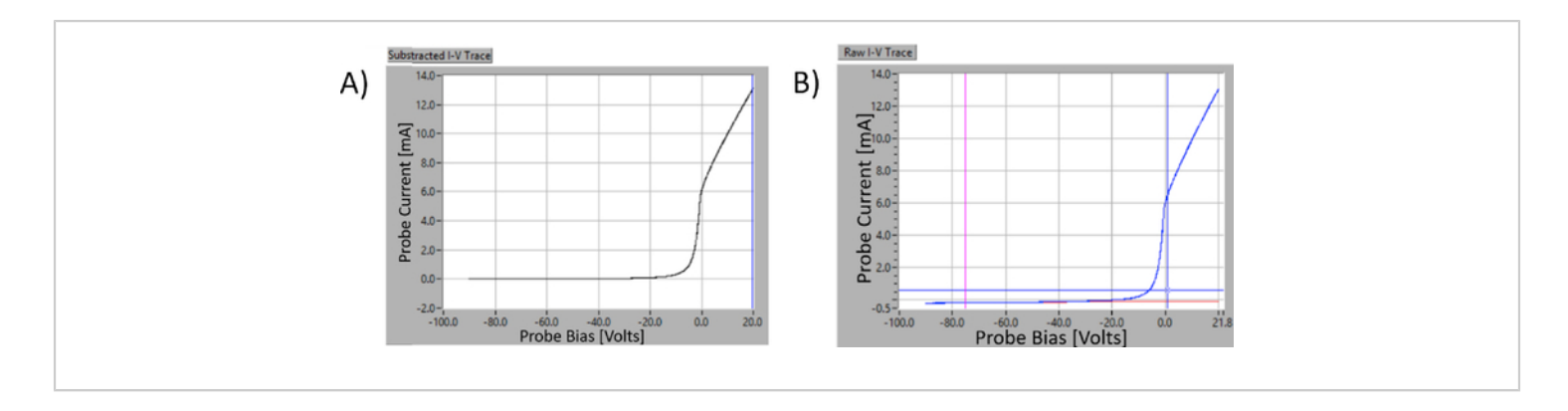


Figure 12: The difference between the probe current and the electron current collected by a planar Langmuir probe. A) Sample of collected current vs. probe bias. The ion saturation current is linearly fitted from -85 V to -65 V. B) I-V trace after the ion current subtracted Please click here to view a larger version of this figure.

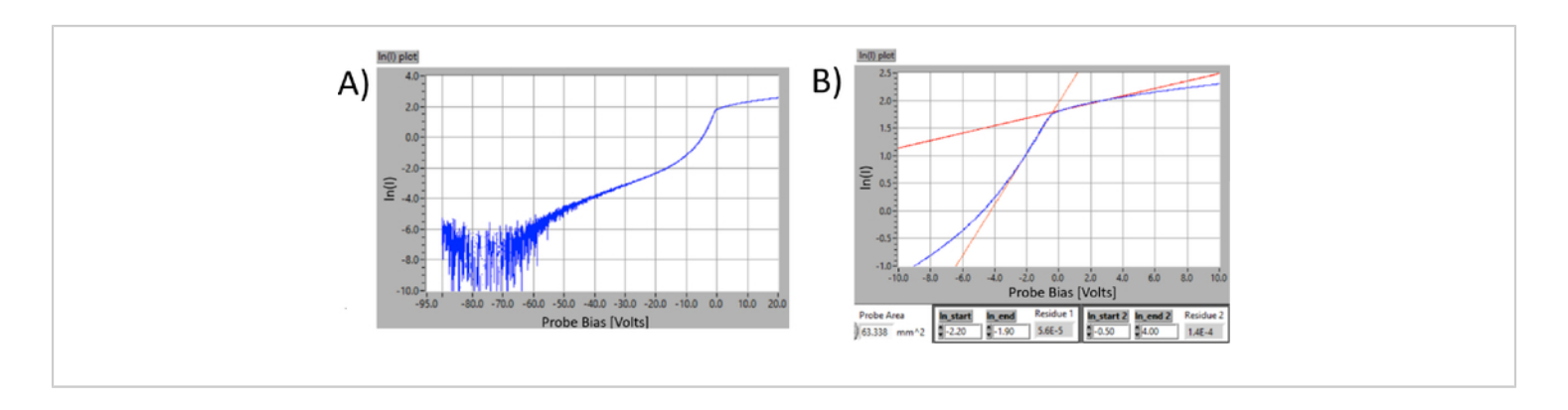
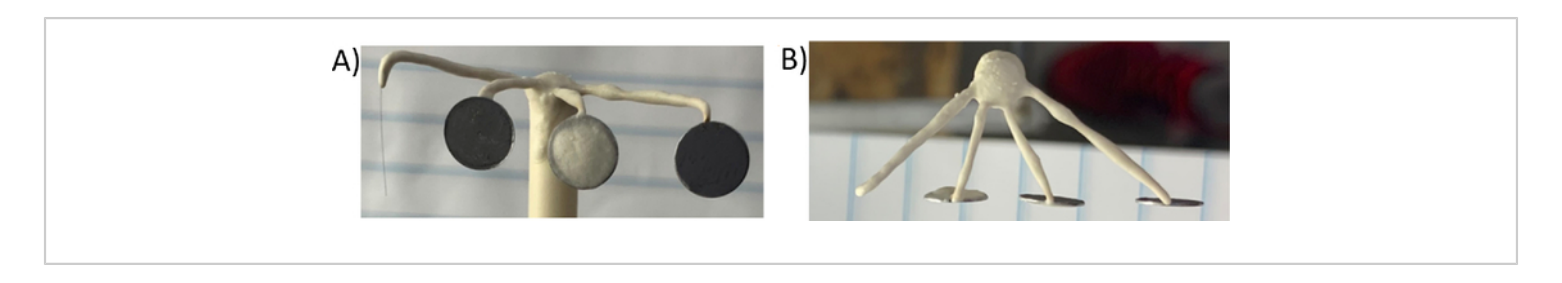


Figure 13: Collected electron currents plotted on semi-log scales permitting electron temper and density

**measurements. A**) a typical I-V trace in a semi-log scale obtained by a ¼" planar disk Langmuir probe B) linear fitting of the transition region. Electron temperature is determined as 2.16 eV from the fitting between -1.9 and -2.2 V. Plasma density is determined by plugging the value of current at the crossing into Eq.3. The plasma potential Vp is determined this way to be about -0.4 V by locating the "knee", which is the location where two fitting lines cross. A more accurate method of measuring the plasma potential was shown in figure 3. Please click here to view a larger version of this figure.





**Figure 14: Multi-tip Langmuir probe detail. A)** front view and **B)** top view of multi-tip Langmuir probe. The system (from left to right) consists of a cylindrical Langmuir probe, a 2-sided planar Langmuir probe, the planar Langmuir probe covered by ceramic paste in the front, the planar Langmuir probe covered in the back. Please click here to view a larger version of this figure.

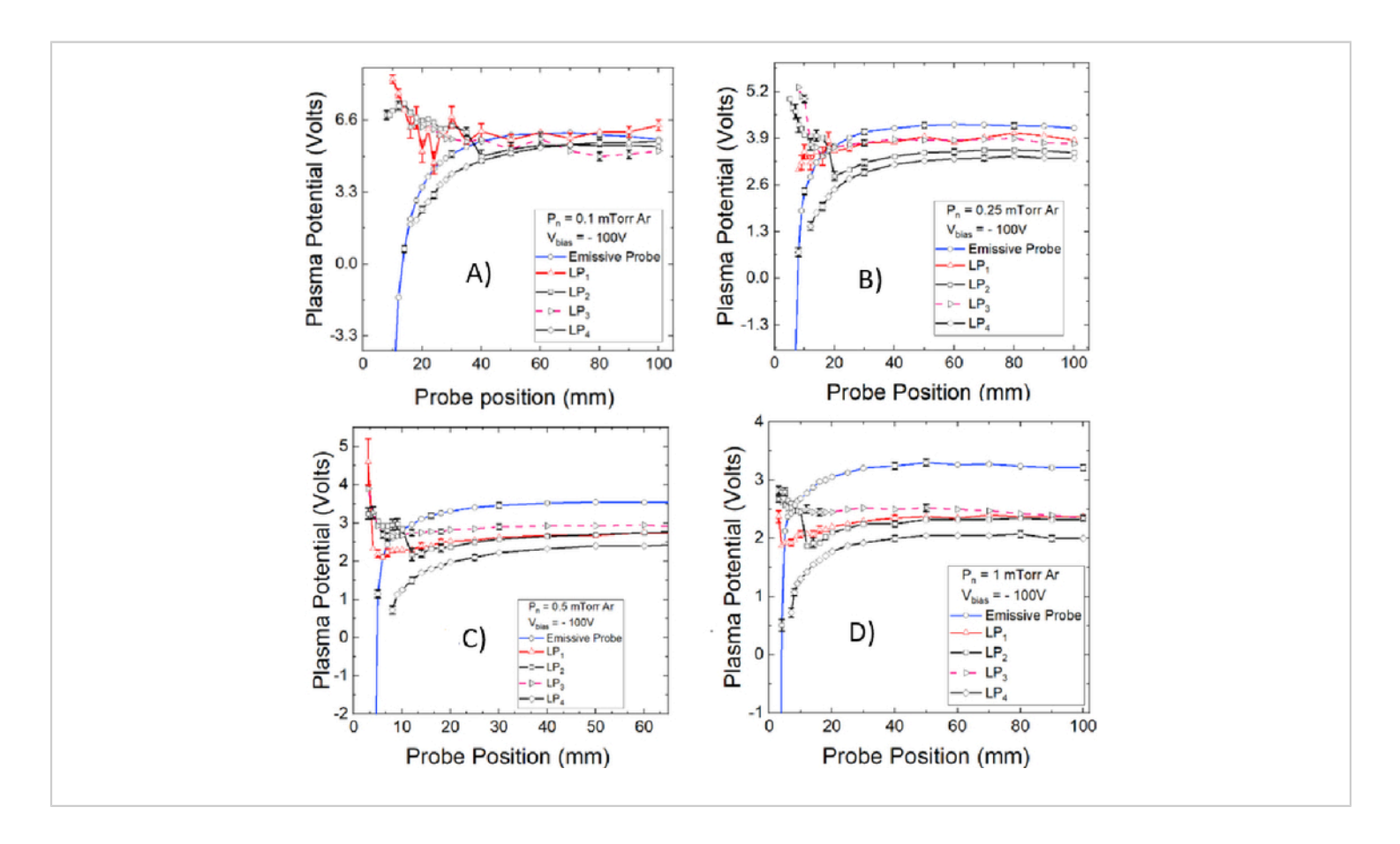


**Figure 15:** Results comparing various Langmuir probes to emissive probe measurements of the plasma potential near a plasma boundary. Plasma potential profiles for four different Langmuir probe configurations, and for an emissive probe, are displayed for four different neutral pressures; (**A**) 0.1 mTorr - (**D**) 1.0 mTorr. The boundary plate which created the sheath structure in the plasma was biased at -100 Volts. The discharge current was kept at 1.0 Amp. This panel of figures is adapted from Ref. 23. Please click here to view a larger version of this figure.



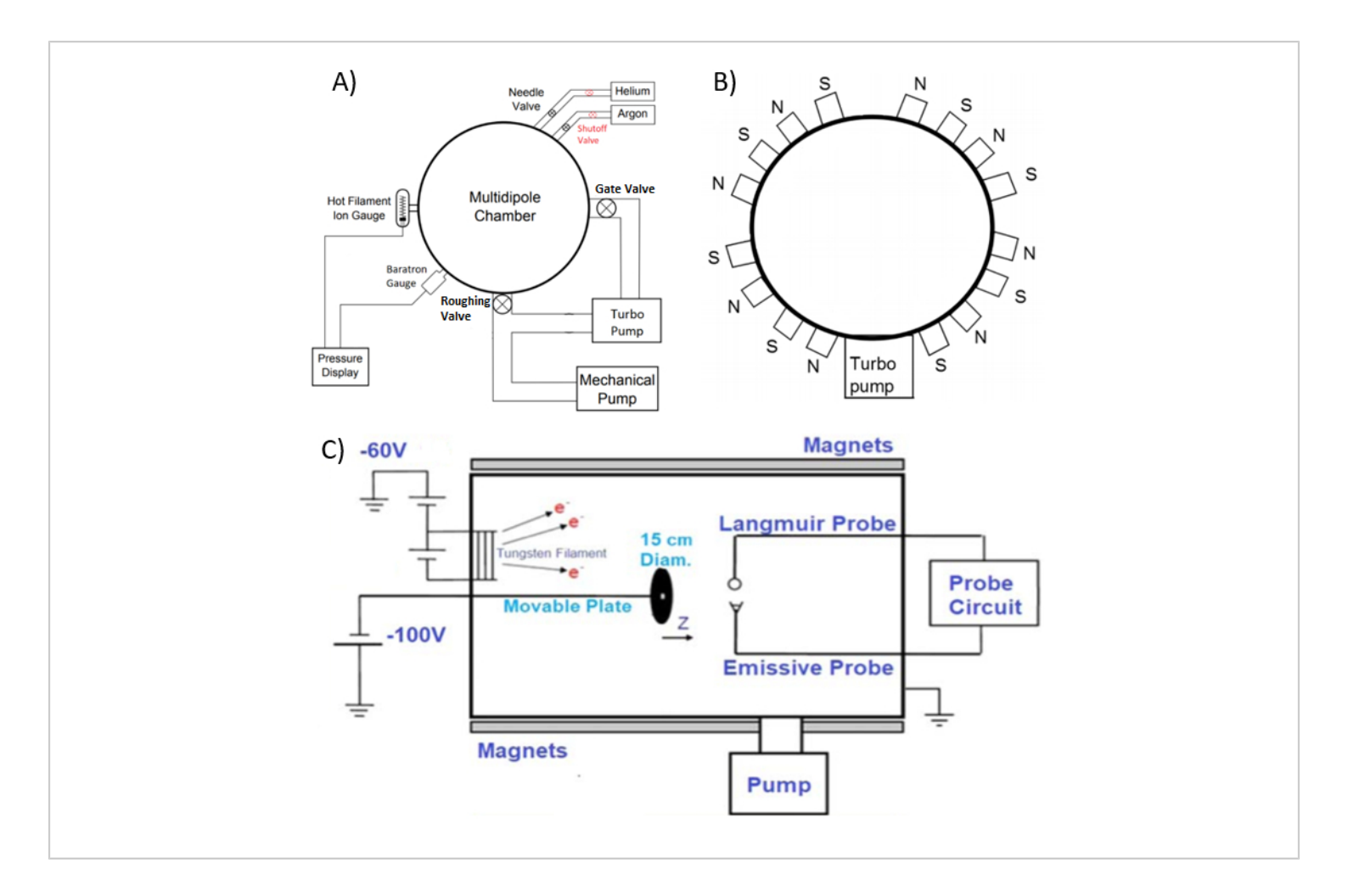


Figure 16: Vacuum Chamber pumping scheme, magnetic confinement, and experimental design set up. The schematic of **A**) vacuum system and **B**) cross section of the multidipole chamber showing rows of magnets that help to confine thermionically emitted electrons, which are shown in **C**) being accelerated to the chamber wall so as to create ionization collisions with the neutral gas atoms, to make and confine the plasma. This figure was in part adapted from ref. 23.



P <sub>n</sub> (mTorr)	T <sub>e</sub> (eV)	n <sub>e</sub> (10 <sup>14</sup> m <sup>-3</sup> )	λ <sub>debye</sub> (m)	dCF (m)
0.1	4.0 ± 0.1	3 ± 2	0.00086	0.0076
0.25	1.9 ± 0.1	10 ± 2	0.0003	0.0051
0.5	1.3 ± 0.1	22 ± 2	0.00018	0.0041
1	1.0 ± 0.1	39 ± 2	0.0001	0.003

Table 1: Plasma parameters for the experiments described in ref. 23, neutral pressure, electron temperature and density, Debye length, and Child- Langmuir length.

Supplemental Figure 1: Filaments for thermionic emission. A) The heating filament array and B) the wire setup on the chamber door. Please click here to download this figure.

Supplemental Figure 2: Boundary plate support wire. Side view of the boundary plate setup from the vacuum viewport. Because of the laser beam dump welded onto the plate, the plate is heavy and needs support from above to maintain its orientation. The angle of the boundary plate is controlled by the length of the wire. The wire itself is attached to an empty Langmuir probe shaft admitted from a flange on the top of the chamber. Please click here to download this figure.

Supplemental Figure 3: Boundary plate bias supply. Bias supply setup for the boundary plate, used to provide a negative bias leading to a sheath structure in the plasma surrounding the boundary plate. Please click here to download this figure.

Supplemental Figure 4: Tube fittings for a rotatable and translatable vacuum seal against the probe shaft. Tube fittings that come with O-rings are readily available and may

be used for rotatable and translatable vacuum seals against a polished cylindrical tube. They can be improved upon with light machining to increase the inner diameter on the side opposite to the vacuum chamber. It is useful to order a brass fitting. Ferrules for ¼" tubing are used to separate 2 O-rings fit into the bore and compressed with the Cajon end nut and pusher, permitting the tube to twist and translate axially while maintaining the vacuum seal. The O-rings are lightly greased with vacuum grease. Please click here to download this figure.

Supplemental Figure 5: Langmuir probes for on-axis measurements, but which enter the vacuum chamber off-axis. Langmuir probe for smaller chambers before all joints sealed with ceramics. A single-bore alumina tube is inserted into the probe shaft until it bottoms out. Please click here to download this figure.

Supplemental Figure 6: BNC vacuum seal scheme. A) A vacuum sealed BNC to KF feedthrough is used to complete the vacuum seal for the probe (double and quad BNC connectors may also be purchased). B) A brass tube to pipe thread fitting may be used to connect to a KF fitting that completes the attachment as shown. Also note that BNC to KF feedthroughs are available with 2 and 4 BNC connectors.



Custom flanges for emissive probes that require 2 BNC connectors, such as those used at UW-Madison, can be avoided if desired. Please click here to download this figure.

Supplemental Figure 7: The difference between raising or lowering the heating currents, consecutively. Inflection point technique to the limit of zero emission by A) high to low heating and B) low to high heating. The pressure is 0.25 mTorr, probe position is 30 mm from the boundary plate, which is biased at -90 Volts. The inflection points of high to low heating have less spread around the fitted line. Please click here to download this figure.

## **Discussion**

Langmuir probes are used for particle flux measurements in an extraordinarily wide range of plasma densities and temperatures, from space plasmas in which the electron density is just a few particles 10<sup>6</sup> m<sup>-3</sup> to the edge region of fusion plasmas where the electron density is more like a few times 10<sup>20</sup> m<sup>-3</sup>. Moreover, electron temperatures between 0.1 and a few hundred eV's have been diagnosed with Langmuir probes. Langmuir probes are often used to measure plasma density and temperature. Finding the electrostatic plasma potential is intimately related to obtaining those two measurements. Emissive probes, on the other hand, are typically used solely to measure the plasma potential, and are of use in an even wider range of plasma parameters. This work describes in detail how to build and use both the Langmuir probes and the emissive probes in a laboratory setting in which a vacuum chamber is used to create and confine the plasma of interest, and discusses critical limitations to the use of Langmuir probes with respect to their use in measuring plasma potentials accurately near plasma boundaries where sheaths and presheaths form.

More rigorous steps of analyzing emissive probe I-V traces to obtain the plasma potential using the inflection point method in the limit of zero emission are discussed by Smith et al.<sup>27</sup>. The user digitally controls the number of heating currents. one of which must be zero, and collects an I-V characteristic just like that described for Langmuir probes, for each heating current. By comparing the ion branch of I-V characteristics for the 'cold sweep', that is, for zero heating current, to all the other characteristics (with positive heating currents), one can deduce to analog conversion Ic, collected current, and Ie, emission current, respectively. The I-V characteristics are smoothed and differentiated, and then the dl/dV curve is also smoothed, and plotted vs. VB. The bias voltages of the maxima of dl/dV curves, which are the inflection points of the I-V traces, are calculated, and then used to plot the ratio I<sub>P</sub>/ I<sub>C</sub> vs. V<sub>infl</sub> (bias voltage of probe at the inflection point). This plot is fit with a linear extrapolation to the bias voltage where  $l_{\rho}/l_{c}$  goes to zero, and this bias voltage determines  $\Phi$ . This procedure is sometimes called the 'inflection point in the limit of zero emission technique'.

Critical steps to building both probes are explained in detail, particularly drawing attention to vacuum seals that permit the probe shafts to be rotated and translated so that the probe tips may be positioned as needed by the researcher. We have indicated where suitable parts could be purchased by particular vendors, and where in-house machining may be required. We have also outlined the basic steps of analysis, more as a process of application of probe theory than as a software-dependent version of computational coding steps, recognizing that each lab may have different computational tools at their disposal.

Langmuir probes, as is true of any diagnostic, have important limitations, some of which are central to the physics questions



we have pursued in this comparison of probe techniques, a comparison which may be briefly summarized as follows: in relatively low temperature, low pressure plasmas, less than 10 eV. less than a few tenths of Pa of neutral pressure, planar and cylindrical Langmuir probe measurements of potential differ from the true plasma potential in the quasineutral presheath. But they have other limitations as well. The Langmuir probe technique is sensitive to plasma flows, and depending on whether the flow is signal or noise, this sensitivity may or may not be a limitation. Further, there can be problems with secondary electron emission, problems with plasma collisionality in higher pressure plasma, problems with ionization if biased too widely, and so forth. Emissive probes of course are not sensitive to plasma flows which make them superior to Langmuir probes in the measurement of plasma potential near boundaries where sheaths form concomitant with ion flows to the boundary. An active area of research regarding emitting surfaces at the boundary of plasma pursues the possibility of inverse sheaths<sup>28</sup> that might form if emission is sufficiently strong, and if the virtual cathode that can form around the emitting surface can indeed trap ions. There is some evidence that suggests inverse sheaths<sup>29</sup> could, where they form, cause emissive probes to float above the local plasma potential. Recent experiments with strongly emitting emissive probes in higher pressure plasma (Pn > 3 mTorr) than that of the experiments reported here to some extent corroborates<sup>30</sup> this view. However, for low pressure, low temperature plasma, with modest heating currents, it appears that the inflection point technique in the limit of zero emission is not affected by this sort of phenomena. Finally we mention one last limitation common to both probe techniques, namely, that if the plasma is too dense and hot the probes cannot mechanically survive 13, leading to the upper limits quoted in the introduction.

# **Disclosures**

The authors have nothing to disclose.

# **Acknowledgments**

This work was partially funded by the U.S. Department of Energy (DOE), through grantDE-SC00114226, and the National Science Foundation through grants PHY-1464741, PHY-1464838, PHY-1804654, and PHY-1804240

## **Tribute to Noah Hershkowitz:**

Noah Hershkowitz made groundbreaking contributions to plasma physics while earning the respect and admiration of his colleagues and students, both as a scientist and a human being. "Physics," he once explained, "is like a jigsaw puzzle that's really old. All the pieces are worn down. Their edges are messed up. Some of the pieces have been put together in the wrong way. They sort of fit, but they're not actually in the right places. The game is to put them together the right way to find out how the world works. He died on November 13, 2020, at age 79.

### References

- Godyak, V. A., Alexandrovich, B. M. Comparative analyses of plasma probe diagnostics techniques. *Journal of Applied Physics*. 118, 233302 (2015).
- Gurnett, D.A. et al. The Cassini Radio and Plasma wave investigation. Space Science Reviews. 114, 395-463 (2004).
- Olson, J., Brenning, N., Wahlund, J. E., Gunell, H. On the interpretation of Langmuir probe data inside a spacecraft sheath, *Review of Scientific Instruments*. 81, 105106 (2010).



- Lebreton, J.P. et al. The ISL Langmuir probe experiment processing onboard DEMETER: Scientific objectives, description and first results. *Planetary and Space Science*. 54, 472-486 (2006).
- Godyak, V. A., Piejak, R. B., Alexandrovich, B. M. Measurements of electron energy distribution in lowpressure RF discharges. *Plasma Sources Science and Technology*. 1, 36-58 (1992).
- You, K. H. et al. Experimental and computational investigations of the effect of the electrode gap on capacitively coupled radio frequency oxygen discharges. *Physics of Plasmas.* 26, 013503 (2019).
- Sobolewski, M. A., Kim, J.H. The effects of radiofrequency bias on electron density in an inductively coupled plasma reactor. *Journal of Applied Physics*. 102 (11), 113302 (2007).
- Godyak, V. A., Piejak, R. B., Alexandrovich, B. M. Electron energy distribution function measurements and plasma parameters in inductively coupled argon plasma. Plasma Sources Science and Technology. 11, 525-543 (2002).
- Leonard, A. W., Plasma detachment in divertor tokamaks. Plasma Physics and Controlled Fusion. 60, 044001 (2018).
- Loarte, A. et al. Plasma detachment in JET Mark I divertor experiments. *Nuclear Fusion*. 38, 331-371, (1998).
- Matthews, G. F. Tokamak plasma diagnosis by electrical probes. *Plasma Physics and Controlled Fusion*. 36, 1595-1628 (1994).
- Langmuir, I. The pressure effect and other phenomena in gaseous discharges. *Journal of the Franklin Institute*.
   196 751-762 (1923).

- Hutchinson, I. H. Principles of Plasma Diagnostics. 2nd.
   Ed. Cambridge University Press. Cambridge UK (2002).
- Hershkowitz, N. How Langmuir Probes Work. In *Plasma Diagnostics Volume 1 Discharge Parameters and Chemistry*. Edited by Auciello, O. and Flamm, D. L., 114-238, Academic Press, Boston (1989).
- Lee, H. C., Lee, J. K., Chung, W. C. Evolution of the electron energy distribution and E-H mode transition in inductively coupled nitrogen plasma. *Physics of Plasmas.* 17, 033506 (2010).
- Amemiya, H. Plasmas with negative ions-probe measurements and charge equilibrium. *Journal of Physics D: Applied Physics.* 23, 999 (1990).
- Andreu, J., Sardin, G., Esteve, J., Morenza, J., L. Filament discharge plasma of argon with electrostatic confinement, *Journal of Physics D: Applied Physics.* 18, 1339-1345 (1985).
- Bohm, D. Minimum Kinetic Energy Requirement for a Stable Sheath. In *The Characteristics of Electrical Discharges in Magnetic Fields*. Edited by Guthrie, A. and Wakering R. K., McGraw-Hill (1949).
- 19. Chen, F. F. Introduction to Plasma Physics and Controlled Fusion, 3rd. Ed. Springer Switzerland (2016).
- Sheehan, J.P., Hershkowitz, N. Emissive probes.
   Plasma Sources Science and Technology. 20 063001 (2011).
- Barnat, E., V., Laity, G., R., Baalrud, S., D. Response of the plasma to the size of an anode electrode biased near the plasma potential. *Physics of Plasmas.* 21, 103512 (2014).
- Mausbach, M. Parametrization of the Laframboise theory for cylindrical Langmuir probe analysis. *Journal of*



- Vacuum Science and Technology A. 15 2923-2929 (1997).
- 23. Li., Peixuan, Hershkowitz, N., Wackerbarth, E., Severn, G. Experimental studies of the difference between plasma potentials measured by Langmuir probes and emissive probes in presheaths. *Plasma Sources Science and Technology.* 29, 025015 (2020).
- Goeckner, M. J., Goree, J., Sheridan, T. E. Measurements of ion velocity and density in the plasma sheath. *Physics of Fluids B: Plasma Physics.* 4, 1663-(1992).
- 25. Lee, D., Hershkowitz, N., Severn, G. D. Measurements of Ar<sup>+</sup> and Xe<sup>+</sup> velocities near the sheath boundary of Ar-Xe plasma using two diode lasers. *Applied Physics Letters.* **91**, 041505 (2007).
- Yan, S., Kamal, H., Amundson, J., Hershkowitz, N. Use of emissive probes in high pressure plasma. *Review of Scientific Instruments*. 67 (12), 4130-4137 (1996).
- Smith, J. R., Hershkowitz, N., Coakley, P. Inflection-point method of interpreting emissive probe characteristics, *Review of Scientific Instruments*. 50, 210-218 (1979).
- Campanell, M. D., Umansky, M. V. Strongly Emitting Surfaces Unable to Float below Plasma Potential. Physical Review Letters. 116, 085003 (2016).
- Kraus, B. F., Raitses, Y., Floating potential of emitting surfaces in plasmas with respect to the space potential. *Physics of Plasmas.* 25, 030701 (2018).
- Yip, C-S., Jin, C, Zhang, W., Xu, G. S., Hershkowitz,
   N. Experimental investigation of sheath effects on I–
   V traces of strongly electron emitting probes. *Plasma Sources Science and Technology*. 29, 025025 (2020).